Polymer 50 (2009) 1526–1532

Contents lists available at ScienceDirect

Polymer

journal homepage: www.elsevier.com/locate/polymer

Porous epoxy monolith prepared via chemically induced phase separation

Jianhua Li, Zhongjie Du, Hangquan Li, Chen Zhang*

The Key Laboratory of Beijing City on Preparation and Processing of Novel Polymer Materials, Beijing University of Chemical Technology, No. 15, BeiSanhuan East Road, Chaoyang District, Beijing 100029, PR China

ARTICLE INFO

Article history:
Received 18 November 2008
Received in revised form
25 December 2008
Accepted 22 January 2009
Available online 29 January 2009

Keywords:
Porous epoxy resin
Chemically induced phase separation
Morphology

ABSTRACT

Macroporous epoxy monolith was prepared via chemically induced phase separation using diglycidyl ether of bisphenol A (DGEBA) as a monomer, 4,4′-diaminodiphenylmethane (DDM) as a curing agent, and epoxy soybean oil (ESO) as a solvent. The morphology of the cured systems after removal of ESO was examined using scanning electron microscopy, and the composition of epoxy precursors/solvent for phase inversion was determined. The phase-separation mechanism was deduced from the optic microscopic images to be spinodal decomposition. The pore structure of the cured monolith was controlled by a competition between the rates of curing and phase separation. The ESO concentration, content of curing agent, and the curing temperature constituted the influencing factors on the porous morphology. The average pore size increased with increasing ESO concentration, increasing curing temperature, and decreasing the content of curing agent.

1. Introduction

Porous polymers, with the advantages of low density, good thermal and electric insulation, and high specific surface, have been found wide applications in foams, membranes, filters, chromatography media, and solid supports. Those with pore size on the order of micrometers are also of interest for applications in catalysis, sensors, size- and shape-selective separation media, adsorbents, and scaffolds [1,2] for bone and tissue in medical applications.

A number of methodologies and technologies have been reported for preparing porous polymers, such as fiber bonded nonwoven, thermally and chemically induced phase separation, freeze drying, gas foaming, porogen leaching, fused deposition modeling, and electrospinning. Chemically induced phase separation (CIPS) [3–5], also known as "polymerization induced phase separation (PIPS)" [6] or "reaction induced phase separation (RIPS)" [7–9], was first proposed by Kiefer in 1996. With the development of curing process, the uniform precursor system undergoes a phase separation into a polymer-rich continuous phase and a solvent-rich droplet phase. The solvent-rich droplets will subsequently grow and merge into each other. After extraction of the solvent, a porous structure is obtained. In order to achieve this, the solvent employed should be a moderately good one for the reactive precursors, yet a non-solvent for the cured network.

Kiefer et al. [3] have used the low molecular weight liquids, hexane and cyclohexane, as the solvents for epoxy precursors, and a nucleation and growth mechanism (NG) was observed. They also studied the effect of chemical nature of the solvent, solvent concentration, and curing temperature on the final porous morphology. Loera et al. [10] have successfully produced controlled porous epoxy thermosets obtained by the thermal oxidative degradation of PVME via PIPS. Analyzing quantitatively by transmission electron microscopy, they have identified the morphology of closed and open cells, bi-continuous percolation canals, which are dependent on the content of thermoplastics and the phase-separation mechanism. Guo et al. [11] prepared porous epoxy resin on the order of 100–300 nm with the removal of a hydroxyl-functionalized hyperbranched polymer (HBP). The phase morphology was observed to be dependent on the composition.

For environmental concerns, the use of small molecular weight solvents should be avoided. Epoxy soybean oil (ESO) was chosen in this work as a solvent for epoxy precursors for biodegradable property and lower cost. The influencing factors on the porous morphology and phase-separation behavior have been investigated.

2. Experimental

2.1. Materials

Diglycidyl ether of bisphenol A (DGEBA, epoxy equivalent weight, EEW 196), was provided by Wuxi Resin Factory of Blue Star New Chemical Materials Co., China, with a commercial code of E-51.

* Corresponding author. Tel.: +86 10 64445339; fax: +86 10 64428804.
E-mail address: zhangch@mail.buct.edu.cn (C. Zhang).

0032-3861/$ – see front matter © 2009 Elsevier Ltd. All rights reserved.
doi:10.1016/j.polymer.2009.01.049

4,4′-Diaminodiphenylmethane (DDM), was obtained from Sinopharm Chemical Reagent Co., Ltd. Epoxy soybean oil (ESO) was supplied by Shandong Jiqing Chemical Co., Ltd. Acetone was a Beijing Yili Fine Chemicals product. The chemical structure of DGEBA, DDM and ESO is shown in Scheme 1.

2.2. Preparation of porous epoxy monolith

The weight ratio of DGEBA to DDM was based on 1:1 molar ratio of amine protons to epoxy groups. DGEBA and ESO were blended in a vessel at 100 °C to form a homogeneous mixture. Liquid DDM at 93 °C was subsequently added to the mixture with continuous stirring. After the addition of DDM, the system was immediately introduced into a sealed glass tube. The samples were cured at 100 °C for 3 h and post-cured at 130 °C for 6 h. The cured monolith was extracted by acetone for 24 h and finally dried overnight in a vacuum oven at room temperature.

2.3. SEM and OM observation

The morphologies of porous epoxy monolith were characterized by a scanning electron microscopic instrument (SEM, S-4700, Jeol Ltd., Tokyo. Japan) operating at an accelerating voltage of 20 kV. The specimens were cut into a cubic shape about $3 \times 3 \times 3$ mm^3, which were sputtered with gold in argon atmosphere prior to observation. Morphology during the phase separation was obtained by an Olympus BH_2 optical microscope (OM). The samples were placed between two glass cover slips and the temperature was controlled by a Mettler FP82-HT hot stage. Digital micrographs were taken at different cure times by a JVC TK-C1381 CCD camera, controlled by the program Qwin of the Leica Company.

2.4. Image analysis

Image analysis was performed on SEM micrographs of three horizontal cross-sections taken from three different areas of the same sample. The pore size was also measured through the SEM using Image J as a software tool, providing number distribution of the pores. In each measurement more than 100 pores were taken into account.

2.5. Determination of porosity

The porosity of the sample was estimated by the following formula: $P(\%) = (1 - \rho_1/\rho_0) \times 100\%$, with ρ_0 and ρ_1 being the density of dense and porous samples, respectively. Average porosity was obtained based on five measurements.

3. Results and discussion

3.1. Morphology and phase separation

In this work, the solution system was considered a pseudo-binary system as epoxy precursors in a solvent, epoxy soybean oil (ESO). The quantity of the precursors was defined as the sum of DGEBA and DDM.

During the preparation of porous epoxy thermosets via CIPS, phase separation is induced by increasing the molecular weight of epoxy monomers. The final morphology is a result of the competition between the kinetics of phase separation and the continuous advancement in crosslinking [12]. The blend composition and the curing temperature are the main influencing factors and determine the mechanism of chemically induced phase separation, i.e. spinodal decomposition (SD) or nucleation and growth (NG) [13]. During spinodal decomposition, a co-continuous structure is formed, which can break up in small particles dispersed in a matrix. SD occurs at or close to the critical point, where small concentration fluctuations lead to de-mixing. At off-critical regions phase separation occurs through nucleation and growth; in this case large concentration fluctuations are necessary for phase separation.

In this work, the weight ratios of DGEBA/DDM/ESO were set at 100/30/100, 100/30/110, and 100/30/130, with the corresponding system denoted as ESO-100, ESO-110, and ESO-130, respectively.

Fig. 1 shows the SEM morphology of the cured products after removal of ESO. For ESO-100 (Fig. 1a), the discrete vacant holes were distributed in epoxy matrix. In contrast, for ESO-130, a phase-inverted structure occurred, aggregating epoxy spheres (Fig. 1d). ESO-110 constituted the intermediate case, where the sample was composed of two layers [14]: Epoxy microspheres presented the upper layer (Fig. 1b) whereas porous epoxy monolith constituted

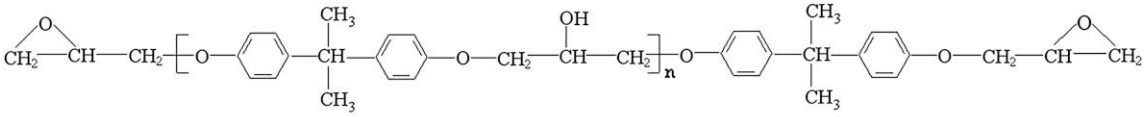

Diglycidyl ether of bisphenol-A (DGEBA)

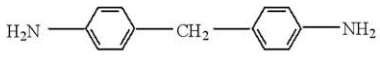

4,4'-Diaminodiphenylmethane (DDM)

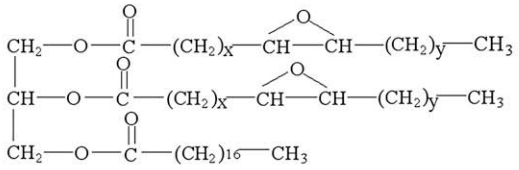

Epoxy soybean oil (ESO)

Scheme 1. Chemical structure of DGEBA, DDM and ESO.

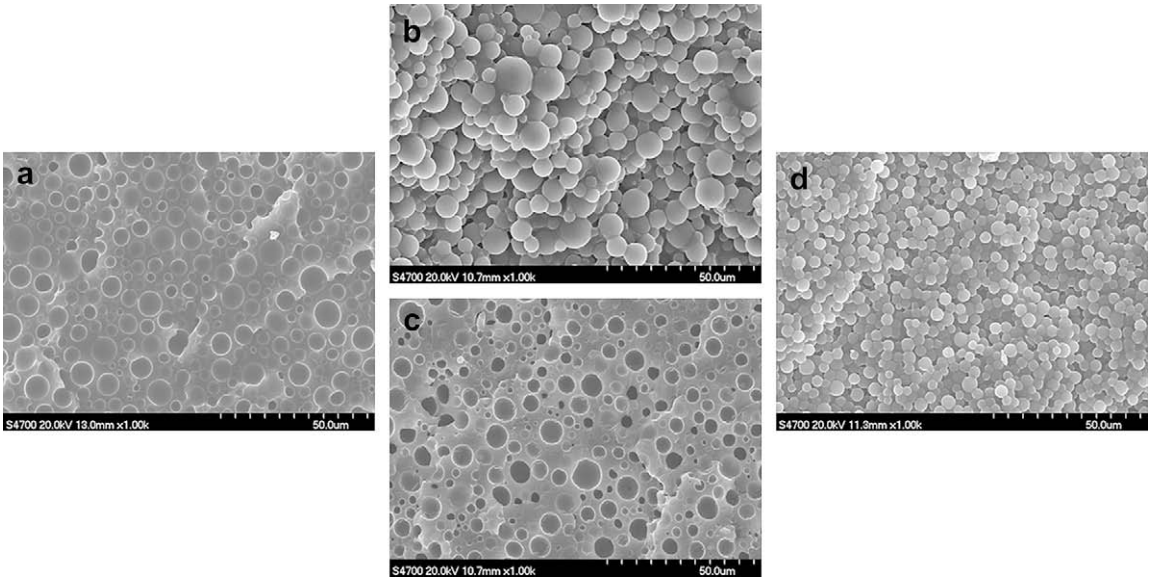

Fig. 1. SEM micrographs of epoxy monoliths after removal of ESO, cured for 3 h at 100 °C and post-cured for 6 h at 130 °C: (a) ESO-100, (b) and (c) ESO-110, and (d) ESO-130.

the lower one (Fig. 1c). One may conclude that the phase structure of the cured epoxy monolith was controlled by the composition, with precursors/solvent = 55/45(w/w) being a threshold. At lower solvent content, a porous structure was observed, whereas at higher solvent content, epoxy particles were obtained. Just in the threshold region, where phase inversion occurred, a two-layered structure was observed.

In order to study the mechanism of phase separation, the DGEBA/DDM/ESO system was cured isothermally at 100 °C and viewed with an optical microscope (OM). With the development of curing, the mixture displayed a decreasing transparency and gradually became translucent or opaque, indicating the occurrence of phase separation. Figs. 2 and 3 display OM pictures of ESO-100 and ESO-130 systems, respectively, during isothermal curing.

For ESO-100, a co-continuous structure (Fig. 2a) was observed at 25 min in the early stage of phase separation, which indicated a SD mechanism [15]. After 25 min, this co-continuous structure began to be broken (Fig. 2b) and transformed to an irregular sea–island structure at 35 min (Fig. 2c). Since in this case the solvent content was low, the cured epoxy resin was able to maintain its integrity, with the ESO-rich phase dispersed in the epoxy-rich matrix. With time elapsed, the large droplet was gradually broken into small ones (Fig. 2d). The ESO-rich phase went on refining, resulting in finer ESO particles (Fig. 2e). After 70 min, the dispersed morphology was finally fixed (Fig. 2f).

The phase-separation process in the ESO-130 system was in an inversed mode (Fig. 3). The phase separation also started with SD mechanism; however, the cured epoxy resin became dispersed in

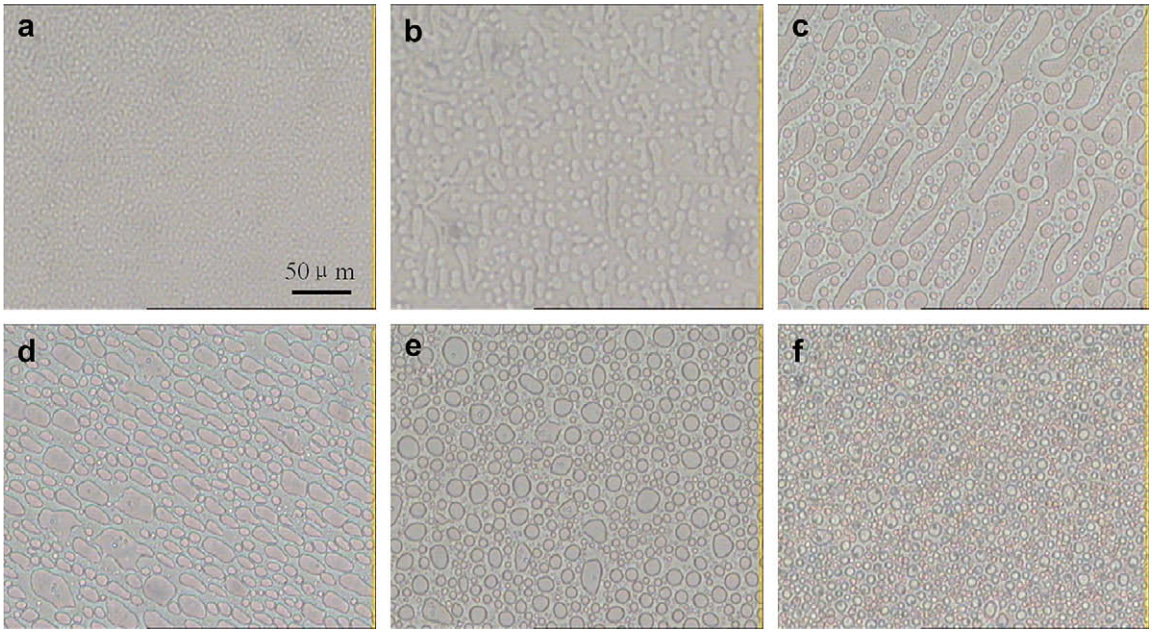

Fig. 2. OM pictures of ESO-100 cured at 100 °C for different time periods: (a) 25 min, (b) 30 min, (c) 35 min, (d) 38 min, (e) 46 min, and (f) 70 min.

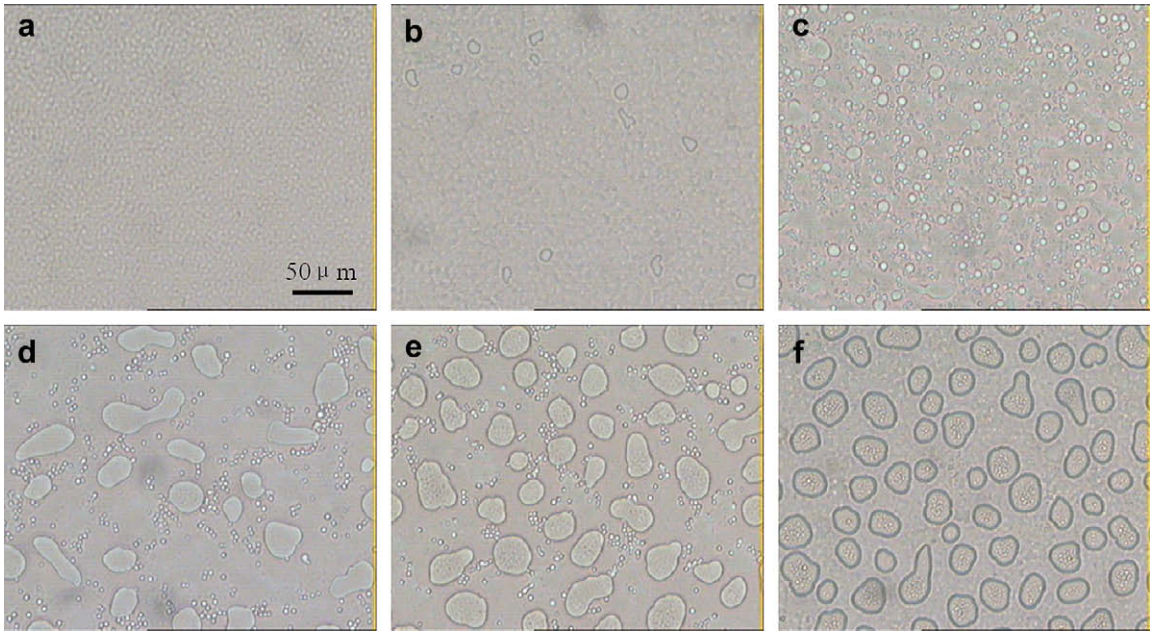

Fig. 3. OM pictures of ESO-130 cured at 100 °C for different time periods: (a) 40 min, (b) 50 min, (c) 60 min, (d) 70 min, (e) 80 min, and (f) 90 min.

the sea of ESO-rich phase. Since the increased ESO amount slowed down the curing reaction, the onset time of the phase separation became delayed, the system remained homogeneous until the co-continuous morphology occurred at 40 min (Fig. 3a). After 40 min, some epoxy domains occurred in the system (Fig. 3b). Subsequently, the co-continuous structure shifted gradually into small epoxy-rich particles dispersed in the ESO-rich phase (Fig. 3c). These particles also underwent ripening (Fig. 3d) and their size

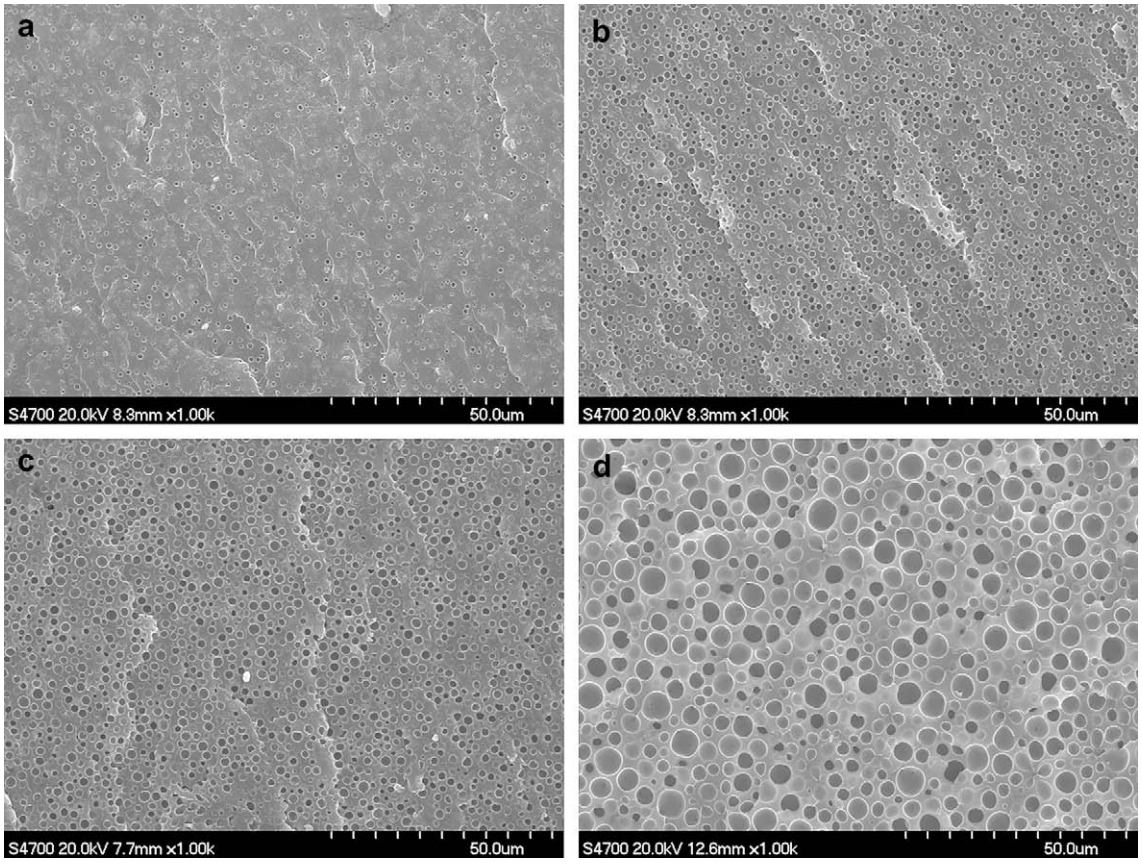

Fig. 4. SEM pictures of porous epoxy monoliths, cured for 3 h at 100 °C and post-cured for 6 h at 130 °C, with different ESO concentrations: (a) 10 wt%, (b) 20 wt%, (c) 30 wt%, and (d) 40 wt%.

Table 1
Average pore size, distribution index, density and porosity of each porous epoxy sample.

Sample	Average pore size (μm)	D_w/D_n	Density (g/cm^3)	Porosity (%)
Porous EP prepared with 10% ESO	1.0	1.04	1.124	2.19
Porous EP prepared with 20% ESO	1.4	1.06	1.097	4.53
Porous EP prepared with 30% ESO	1.8	1.08	1.066	7.31
Porous EP prepared with 40% ESO	4.0	1.11	1.051	8.57

became more uniform by coagulation and breaking (Fig. 3e). After 90 min, the phase-inversion morphology was finally fixed (Fig. 3f). It was clear that the epoxy-rich particles possessed a two-phase structure, in which many ESO-rich droplets dispersed in epoxy matrix.

3.2. Influence of ESO concentration

In order to further explore the effect of solvent concentration, SEM was employed to measure the pore size and its distribution in cured samples with different ESO concentrations. The systems were cured for 3 h at 100 °C and post-cured for 6 h at 130 °C. Typical morphology is shown in Fig. 4.

One may notice that the average pore size increased with increasing solvent concentration. As listed in Table 1, the average diameter of pores increased from 1.0 to 4.0 μm with ESO concentration increased from 10 wt% to 40 wt%.

The pore size distribution was measured via image analysis on SEM. The column graphs (Fig. 5) showed the distributions and the calculated distribution index (D_w/D_n) is listed in Table 1. It was clear that a higher solvent concentration provided not only a larger pore size, but also a broader pore size distribution.

The influence of ESO concentration on the pore size and its distribution could be explained by curing kinetics. With the curing reaction development, the initial homogeneous mixture was separated into an epoxy-rich and an ESO-rich phase. It was obvious that the higher the ESO concentration, the slower the crosslinking of epoxy precursors. In the case of higher solvent content, the ESO-rich droplets had sufficient time and space to grow and merge into each other until the stabilization of the network structure, resulting in larger and non-uniform pores. In the inverse case, the concentration of epoxy precursors was higher, the coagulation of small droplets was limited by the faster formation of epoxy network, the pore size would be smaller and more uniform [16].

The density and porosity of the samples are also shown in Table 1. It could be well expected that the higher the solvent concentration, the lower the density of the monolith and the greater the porosity. Of course, neither density nor porosity followed a linear change with the solvent content. The reason was multi-folded: only part of ESO contributed to the pore formation, that is, during the extraction of ESO, the pores' phase may be subjected to collapse and shrinkage [17,18]; the ESO possessed an epoxy value of 6.0%, it was difficult to measure what a fraction of it took part in the curing reaction. In addition, because of the close-cell structure, quite a fraction of ESO could not be extracted from the monolith [19],

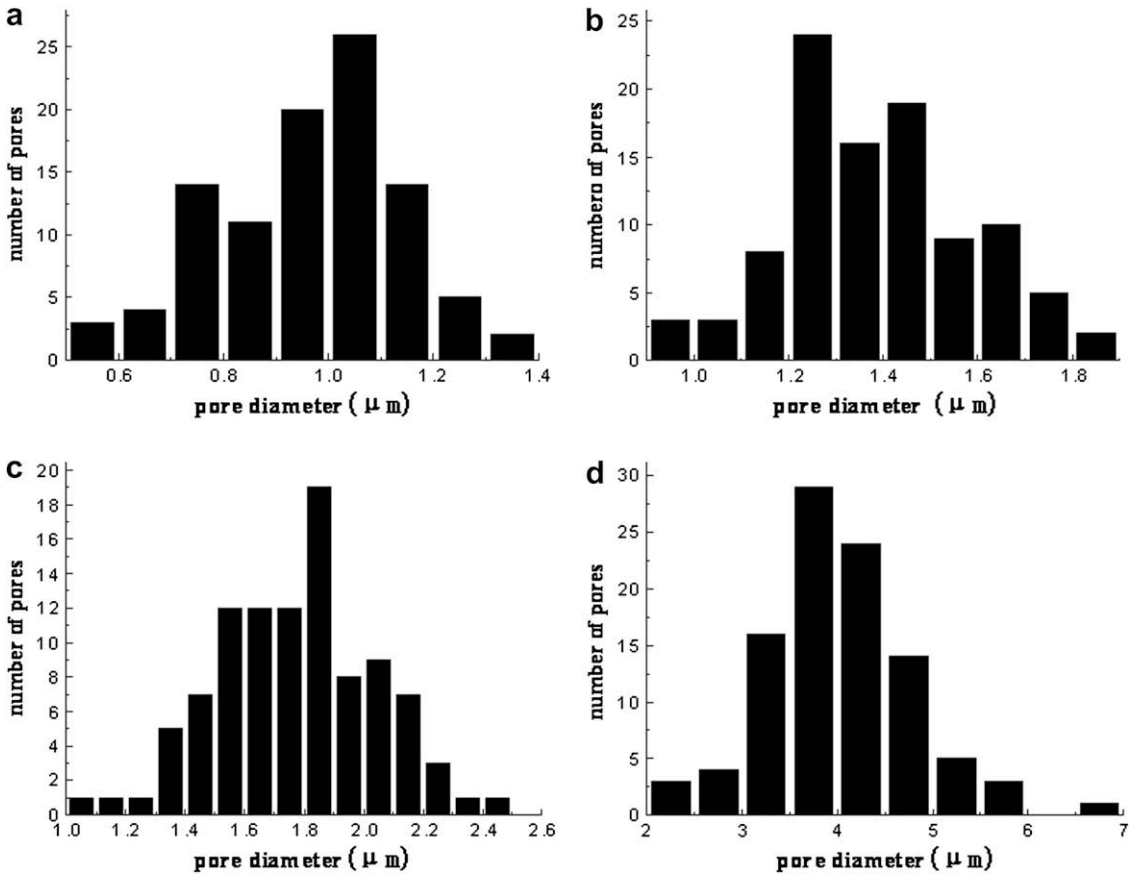

Fig. 5. Pore size distribution for porous epoxy monoliths, cured for 3 h at 100 °C and post-cured for 6 h at 130 °C, with different ESO concentrations: (a) 10 wt%, (b) 20 wt%, (c) 30 wt%, and (d) 40 wt%.

which added the complexity of the change in porosity and density of the monolith.

3.3. Influence of content of curing agent

Since the porous structure was a result of the competition between the kinetics of phase separation and the continuous advancement of crosslinking, the rate of curing reaction played a significant role on the final morphology. Fig. 6 compares the morphology of epoxy monoliths based on the different contents of curing agent, cured at 100 °C for 3 h and post-cured at 130 °C for 6 h. It was clear that the higher the content of curing agent, the smaller the porous structure. Increase in the amount of the curing agent meant increasing the curing rate, and the curing system arrived to the gel point sooner, and smaller pore size was observed.

3.4. Influence of curing temperature

Fig. 7 illustrates the influence of curing temperature on the porous structure. It showed that higher curing temperature resulted in larger pore size. Since the curing temperatures employed in this work were well below the critical temperature, the mechanism

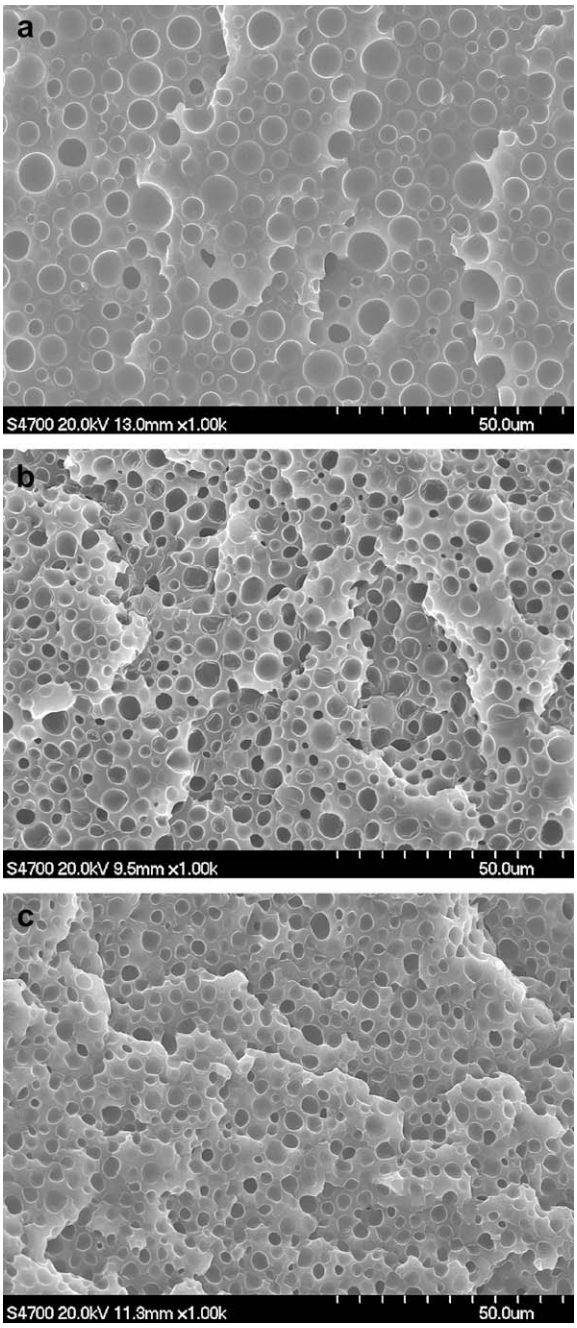

Fig. 6. SEM pictures of porous epoxy monoliths cured for 3 h at 100 °C and post-cured for 6 h at 130 °C. The initial weight ratios of DGEBA/DDM/ESO system were: (a) 100/30/100, (b) 100/50/100, and (c) 100/70/100.

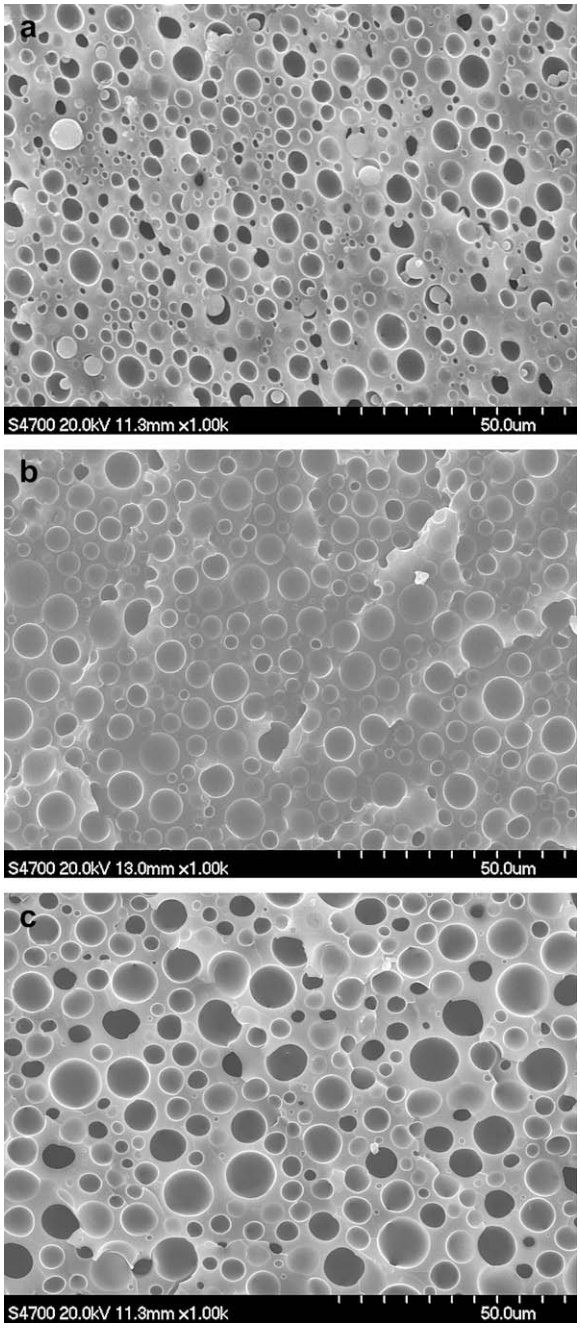

Fig. 7. SEM pictures of porous epoxy monoliths at different curing temperatures: (a) 80 °C, (b) 100 °C, and (c) 120 °C. The initial weight ratios of DGEBA/DDM/ESO system were 100/30/100.

of phase separation would not be changed. However, two competing results would be attributable to the increasing of curing temperature: (i) higher curing rate, which caused the pore size lowering; and (ii) lower system viscosity, which caused the pore size growing. From the results in Fig. 7, one may conclude that the factor of system viscosity constituted the overwhelming one in this case [20].

4. Conclusions

Epoxy soybean oil had been employed as a solvent to prepare macroporous epoxy monolith via chemically induced phase separation. In order to obtain a porous morphology, the weight ratio of precursors/solvent should be higher than 55/45(w/w), otherwise epoxy spheres occurred. Optical micrographs revealed the phase separation via a spinodal decomposition mechanism. With increasing ESO concentration, the porous network exhibited a larger pore size and a broader distribution, and thus a lower density and a higher porosity of the products. The pore structure of the cured monolith was determined by a competition between the rates of curing and phase separation. Higher content of curing agent accelerated the curing rate, resulting in smaller pore size. At higher curing temperature, the phase-separation rate prevailed over the curing rate, and pore size became larger.

References

[1] Safinia L, Mantalaris A, Bismarck A. Langmuir 2006;22(7):3235–42.
[2] Nakanishi K, Amatani T, Yano S. Chem Mater 2008;20(3):1108–15.
[3] Kiefer J, Hilborn JG, Manson JA, Leterrier Y. Macromolecules 1996;29(11):4158–60.
[4] Kiefer J, Hilborn JG, Hedrick JL, Cha HJ, Yoon DY, Hedrick JC. Macromolecules 1996;29(26):8546–8.
[5] Kiefer J, Hilborn JG. Polymer 1996;37(25):5715–25.
[6] Elicabe GE, Larrondo HA, Williams RJJ. Macromolecules 1998;31(23):8173–82.
[7] Borrajo J, Riccardi CC, Williams RJJ, Siddiqi HM, Dumon M, Pascault JP. Polymer 1998;39(4):845–53.
[8] Girard-Reydet E, Sautereau H, Pascault JP, Keates P, Navard P, Thollet G, et al. Polymer 1998;39(11):2269–80.
[9] Oyanguren PA, Frontini PM, Williams RJJ, Vigier G, Pascault JP. Polymer 1996;37(14):3087–92.
[10] Loera AG, Cara F, Dumon M, Pascault JP. Macromolecules 2002;35(16):6291–7.
[11] Guo Q, Harard A, Park Y, Halley PJ, Simon GP. J Polym Sci Part B Polym Phys 2006;44(6):889–99.
[12] Teng KC, Chang FC. Polymer 1993;34(20):4291–9.
[13] Chen JL, Chang FC. Polymer 2001;42(5):2193–9.
[14] Chen F, Sun T, Hong S, Meng K, Han CC. Macromolecules 2008;41(20):7469–77.
[15] Goossens S, Goderis B, Groeninckx G. Macromolecules 2006;39(8):2953–63.
[16] Yang Y, Zhao J, Zhao Y, Wen L, Yuan X, Fan Y. J Appl Polym Sci 2008;109(2):1232–41.
[17] Zhang H, Zhou J, Zhang X, Wang H, Zhong W, Du Q. Eur Polym J 2008;44(4):1095–101.
[18] Lv R, Zhou J, Du Q, Wang H, Zhong W. J Appl Polym Sci 2007;104(6):4106–12.
[19] Ratna D. Polym Int 2001;50(2):179–84.
[20] Bussi P, Ishida H. Polymer 1994;35(5):956–66.